17A.2

ON THE WAVE INDUCED WIND IN THE MARINE ATMOSPHERIC BOUNDARY LAYER

Alvaro Semedo[1,2,(*)], Øyvind Saetra [3] and Anna Rutgersson[1]

1 *University of Uppsala, Uppsala, Sweden*
2 *Risø National Laboratory, Roskilde, Denmark*
3 *The Norwegian Meteorological Institute, Oslo, Norway*

Abstract. Recent field observations and large-eddy simulations have shown that the impact of fast running waves (swell) on the marine atmospheric boundary layer (MABL) might be stronger than previously assumed. In low to moderate wave following winds, swell propagates faster than the mean wind, resulting on increasing values of the wave age (c_p / U). The total stress (momentum flux) above the sea surface will therefore have two major components: the turbulent shear stress, and the wave-induced stress, directed downward and upward, respectively. For sufficiently high wave age val[1]ues, the wave-induced component becomes increasingly dominant, and the total momentum flux will be directed into the atmosphere. Recent field measurements have shown that this upward momentum transfer from the ocean into the atmosphere has a considerable impact on the surface layer flow dynamics and on the turbulence structure of the MABL.The vertical wind profile will no longer exhibit a logarithmic shape, since an acceleration of the air flow near the surface will take place, generating a low level wave-driven wind maximum (a wind jet).The picture that emerges from this feedback process is of momentum being transferred from the wind into the ocean. Part of this momentum will be used to drive ocean currents, but some will be responsible by the wave generation process along storm tracks. As waves propagate away from their generation area as swell, some of the momentum will be returned to the atmosphere in the form of wave-driven winds. A model that reproduces quantitatively and qualitatively the wave following atmospheric flow and the wave generated wind maximum, as seen from measurements, is proposed. The model has no previous assumptions or restrictions on the turbulence structure of the surface layer of the MABL. New parameterizations for the wave-induced stress at the surface (expressed as a function of the wave damping ratio and wave slope) and the variation of the wave-induced stress with height are included in the model.

(*) Corresponding author address:
Uppsala University, Villavägen 16, SE-752 36
Uppsala, Sweden
alvaro.semedo@met.uu.se

1. Introduction

Although it might seam intuitive that fast running waves (swell) arriving on light wind areas will have an impact on the local wind field, this concept had not been devoted the proper attention until Harris (1966) laboratory experiments. During several experiments performed in an indoor wave tank, using a mechanical wave generator, it was noticed that a weak wind immediately above the waves was always present. He assumed that this wave induced flow was the result of an atmospheric stokes drift induced by the underlying waves. Harris (1966) named this phenomenon the “wave-driven wind”.

Observations of the air-sea interaction regime in the presence of swell are relatively rare and sparse. Nevertheless studies in the early 1970s from diferent Soviet ocean campaigns (Volkov 1970; Belinov et al.

1974) and from LakeMichigan (Davidson and Frank 1973), from the Baltic Sea (Smedman et al. 1994, 1999; Rutgersson et al. 2001), and from several campaigns in the Atlantic and Pacific Oceans (Donelan et al. 1997; Grachev and Fairall 2001), have found evidence that the presence of fast running waves during light winds induces an upward momentum flux, directed from the water surface to the atmosphere.

The study from Smedman et al. (1999) was based on observations collected from a tower located on the southern tip of the small island Östergarnsholm, in the Baltic Sea. During periods of strong swell regime, upward directed momentum fluxes were recorded from turbulence sensors. In addition, wind measurements at several levels showed a well defined negative wind gradient above the first measuring level (around 8 meters high above the mean sea level). This negative gradient indicated the presence of a low-level wind maximum in the lower marine atmospheric boundary layer (MABL). These findings were in agreement with what Harris (1966) had already postulated, saying that it would be possible that a wave-driven wind might produce a perturbation on the velocity profile by increasing the wind velocity in the direction of wave propagation at low elevations above the water.

Up until recently the wave-driven wind has been looked at an exotic case, as mentioned by Grachev and Fairall (2001). In spite of being an intriguing process, the dominant idea has been that it only occurs in a thin layer above the water surface, and that it has presumably no impact on the dynamics of the atmosphere (Janssen 2004).

Sullivan (2002) and Rutgersson and Sullivan (2005), using direct numerical simulations (DNS), and Sullivan et al. (2008), using large eddy simulations (LES), investigated the impact of swell on the MABL. Their findings indicate a stronger impact of swell on the MABL in agreement with previous measurements. The impact of swell, was shown both by measurements and simulations, not only to generate a wave-driven wind, but also to influence the overall turbulence structure of the MABL.

Kudryavtsev and Makin (2004) presented numerical solutions from a one-dimensional stationary model for the MABL flow in the presence of swell. In spite of the fact that their model for the wave-induced wind reproduces a low level wind maximum, the height of the maximum is considerably lower than what has been found by Smedman et al. (1999) and Sullivan et al. (2008).

The basic concept behind the wave-driven wind and momentum transfer from waves into the MABL, is that swell waves perform work on the overlying atmosphere as they propagate faster than the wind, producing a forward thrust on the flow. Hence swell looses momentum and energy to the atmosphere as it gradually decays, accelerating the airflow. Under swell influence, the wind profile exhibits a low-level wind maximum and a negative (or constant) gradient from there on, violating the logarithmic wind profile law. The Monin-Obukhov similarity theory cannot be claimed as valid in this situation (Miller et al. 1999; Smedman et al. 2003).

As Hristov et al. (2003) pointed out, the incomplete understanding of the atmosphere-ocean interchanging processes reduces the predictability not only of climate models, but also of weather and wave forecasting models. Swell is known to propagate thousands of kilometers across entire oceans (Snodgrass et al. 1966), crossing the tropics and the equatorial regions where light wind regimes prevail. The picture that emerges from this feedback process is of momentum being transferred from the wind into the ocean at mid and high latitudes, where storms are more frequent. Part of this momentum is used in the wave generation process along storm tracks. As waves propagate away from their generation area as swell, some of this momentum is returned to the atmosphere, mainly at lower latitudes, in the form of wave-driven winds. Therefore a better physical understanding of this process is of considerable interest from a global climatological point of view.

In the present study a model that reproduces qualitatively and quantitatively the wave-induced wind is proposed. The model has no previous assumptions or restrictions on the turbulence structure of the surface layer of the MABL. The model is

presented in section 2., along with the proposal of new parameterizations for the wave-induced stress at the surface (expressed as a function of the wave damping ratio and wave slope), and variation with height. In section 3 some basic results and sensitivity tests of the model are shown.

2. The model

For 2-dimensional stationary flow with no horizontal gradients, it follows from the principle of conservation of momentum that the shear stress is constant in the turbulent boundary layer. The momentum equation then reads

$$\frac{\partial \tau_{tot}}{\partial z} = 0 . \qquad (1)$$

Here, z is the vertical coordinate, which is positive upward and τ_{tot} is the total stress. In the presence of ocean-waves, we will divide the total stress into turbulent shear stress (τ_{turb}) and wave-induced stress (τ_{wave}) (Phillips 1977):

$$\tau_{tot} = \tau_{turb} + \tau_{wave} \qquad (2)$$

Following Kitaigorodskii (1970) the kinematic turbulent and wave-induced stresses are defined as:

$$\tau_{turb} = -\langle u'w' \rangle , \qquad (3)$$

and

$$\tau_{wave} = -\langle \tilde{u}\tilde{w} \rangle . \qquad (4)$$

Here u and v are the longitudinal and vertical components of the flow, the brackets indicate time averaging and the primes and the tilde denote turbulent and wave-induced flow fluctuations, respectively. The turbulent stress will be parameterized as

$$\tau_{turb} = K_m \frac{dU}{dz} , \qquad (5)$$

Where K_m is the turbulent eddy viscosity and U is the mean horizontal wind. The eddy viscosity can be related to the turbulent kinetic energy, b, and the mixing length, l, as

$$K_m = l\sqrt{b} . \qquad (6)$$

Following Kudryavtsev and Makin (2004), we assume a balance between shear production, vertical rate of change of energy flux and dissipation of turbulent kinetic energy is assumed. The turbulent kinetic energy budget is then (Tennekes and Lumley 1972)

$$\tau_{tot} \frac{dU}{dz} + F_w + B - \varepsilon = 0 , \qquad (7)$$

where ε is the energy dissipation and B is the buoyancy term (Kraus and Businger 1994). The wave term in equation (7) is

$$F_w = -\frac{1}{\rho}\frac{d}{dz}\left(\langle \tilde{p}\tilde{w} \rangle\right) . \qquad (8)$$

Here, $\tilde{p}$ is the fluctuating part of the pressure due to the waves and is ρ_a the density of the air. The energy dissipation term can be parameterized as

$$\varepsilon = \frac{b^{3/2}}{l}. \quad (9)$$

Now, combining (1), (2), (4) and (5) we find a differential equation for the mean wind speed,

$$\frac{dU}{dz} = \frac{\tau_{tot} - \tau_{wave}}{K_m}. \quad (10)$$

Similarly, combining equations (5), (6), (7) and (9) yields and equation for the turbulent kinetic energy,

$$b^2 = \left|\tau_{tot}\left(\tau_{tot} - \tau_{wave}\right)\right| + l\sqrt{b}\left(F_w + B\right). \quad (11)$$

Here, the total stress can be negative, i.e upward directed. This will be the case whenever the magnitude of the wave stress is larger than the turbulent stress. The shear production term in equation (7) may therefore become negative. The absolute value of the first term on the right hand side is taken to avoid such negative production of turbulent kinetic energy. If the wave stress is known and the total stress or the wind speed is specified at one vertical level, equations (10) and (11) give the wind velocity distribution with height.

For irrotational waves, the orbital velocity components decay as e^{-2kz}, where k is the wave number. In this case, the vertical and horizontal components are 90 degrees out of phase. The wave stress is then of course zero. When a small amount of work is performed at the surface, the velocity components are slightly phase shifted, as observed in the Large Eddy Simulations (LES) of Sullivan et al. (2008), who found an exponentially decaying wave-induced stress. Here, the wave stress becomes positive or negative, depending on the direction of the energy and momentum fluxes. In this study, it will be assumed that the vertical decay of the velocity components is also exponential when a wave damping is present. The wave stress will then have the form

$$\tau_{wave} = \tau^0_{wave} e^{-2kz}, \quad (12)$$

where τ^0_{wave} is the wave induced stress at the surface.

This surface wave stress can be related to the wave damping thought the rate of work performed at the surface. For one harmonic wave component, the energy per unit area is

$$E = \frac{1}{2}\rho_w g a^2, \quad (13)$$

where ρ_w is the water density, g is the acceleration of gravity and a is the wave amplitude. The rate of change of wave energy caused by a surface stress is proportional to the phase velocity times the stress:

$$\frac{\partial E}{\partial t} = \rho_a c \tau^0_{wave}, \quad (14)$$

where c is the phase velocity. By linear theory, the rate of change of wave energy in decaying waves may be written as

$$\frac{\partial E}{\partial t} = \beta E, \quad (15)$$

Where β is the wave damping coefficient. When waves loose energy and momentum to the mean flow, the swell itself is subject to damping. The wave damping coefficient β represents the wave energy loss transferred into the atmosphere. Using equations (13), (14) and (15), the relation between τ^0_{wave} and β is found to be

$$\tau_{wave}^{0} = -\frac{1}{2}\frac{\beta g a^2}{sc}, \qquad (16)$$

where $s = \rho_a / \rho_w$.

To the lowest order, the wave damping process is governed by a linear instability problem for two dimensional flow described by the Orr-Sommerfeld equation (Saetra 1998). For inviscid flow this equation is reduced to the Rayligh equation. This Rayleigh equation has a singularity at the critical height, where the phase velocity and the mean wind speed are equal. For growing waves, the wave motion experiences a phase shifted in a narrow region around the critical height, inducing a pressure work on the surface and extracting momentum from the mean flow (Miles 1957). The observations by Hristov et al. (2003) are a strong evidence of the critical layer theory as the main agent for wave growth. For swell, the critical layer vanishes and the Rayleigh equation yields only a stable solution. To find the wave damping in this case, the full Orr-Sommerfeld equations must be solved. For this matter the parameterization of the wave damping parameter β remains an opened problem. Although some laboratory experiments have been done (e.g. Doneland (1999), a consensus on the attenuation rate of the energy of fast running waves is still missing.

As τ_{wave}, the energy flux in equation (8) is also related to the rate of work:

$$-\left\langle \tilde{p}\tilde{w} \right\rangle = \rho_a c \tau_{wave}^{0} e^{-2kz}. \qquad (17)$$

Accordingly, the pressure perturbation term in equation (7) becomes

$$F_w = -2kc\tau_{wave}^{0} e^{-2kz}. \qquad (18)$$

A simplification of the model can be presented by assuming an eddy viscosity that is increasing linearly with height from the surface as

$$K_{lm} = l u_*, \qquad (19)$$

where

$$u_* = \sqrt{|\tau_{tot}|}. \qquad (20)$$

and the mixing length is

$$l = \kappa z, \qquad (21)$$

where $\kappa = 0.41$ is the von Karman constant. The solution to equation (10) can then be written as

$$U(z) = \frac{\tau_{tot}}{u_* \kappa} ln\left(\frac{z}{z_o}\right) - \frac{\tau_{wave}^{0}}{u_* \kappa} \int_{z_o}^{z} \frac{e^{-2kz}}{z} dz, \qquad (22)$$

where z_0 is the aerodynamic roughness length. In addition to the traditional logarithmic solution, a swell induced term is now present.

3. Results- general behavior of the model

In this section general model results, along with some model sensitivity tests, are presented. Both wind velocity profiles from equations (10) and (22) are investigated using the eddy viscosity with vertical distribution of TKE (K_m) from equation (6), and the linearly increasing with height eddy viscosity (K_{lm}) from equation (19), respectively. The atmospheric input parameters to the model are an upward directed momentum flux (or total stress)

$\tau_{tot} = -10^{-2}\, m^2 s^{-2}$, a wave damping coefficient $\beta = -5 \times 10^{-5}\, s^{-1}$ (following the same order of magnitude as in Kudryavtsev and Makin (2004)), and a constant roughness length $z_0 = 10^{-5}\, m$. A monochromatic wave field, with amplitude $a = 1m$ and wave number $k = 0.1 m^{-1}$ (resulting in a wave phase speed $c = 9.9 ms^{-1}$) is also used. Neutral stratification is assumed, so that the buoyancy term on equation (11) can be neglected. From these input parameters, the values at the surface for the wave-induced stress, from equation (12), and wave energy flux, from equation (16) are $\tau^0_{wave} = -2.12 \times 10^{-2}$ and $F^0_{wave} = -1.72 \times 10^{-1}$, respectively. The two wind speed profiles are shown in figure 1. A distinctive wave-induced low level wind maximum is present in both cases. The profile calculated using K_{lm} (dot-dashed line) has a more pronounced bulge and higher wind speed at the maximum than the profile evaluated with the K_m formulation. The heights of the wind maxima are the same for both cases ($z = 3.3\, m$), following equation (10). The wind speeds at the maxima are $2.4 ms^{-1}$ and $3.5 ms^{-1}$, for the formulations with K_m and K_{lm}, respectively.

The vertical profiles for the two eddy viscosity formulations are shown in figure 2 (dashed and dot dashed lines for K_m and K_{lm}, respectively). The inclusion TKE on the K_m formulation results on an enhancement of the eddy viscosity up to about 25 meters, compared with the linearly increasing with height K_{lm} formulation. The immediate result is a vertical diffusion of momentum. This turbulence diffusion leads to a less pronounced wind speed maximum, as can be seen in figure 1. The lower value of wind speed at the maximum is also related to the diffusion of momentum.

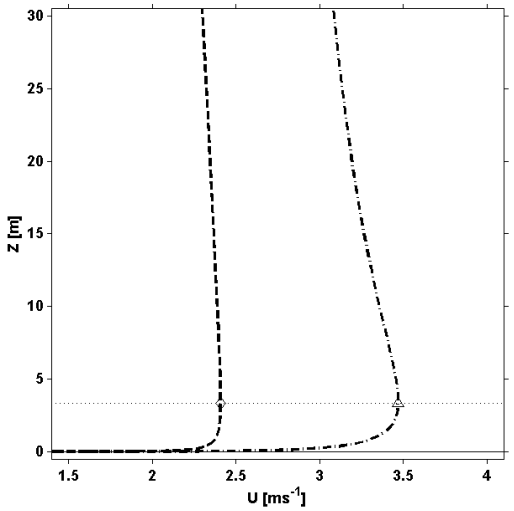

Figure 1. Wind profiles with the K_m (dashed line) and K_{lm} (dot-dashed line) formulations. The heights of the wind maxima (circle for the K_m formulation and triangle for the K_{lm} formulation) are the same.

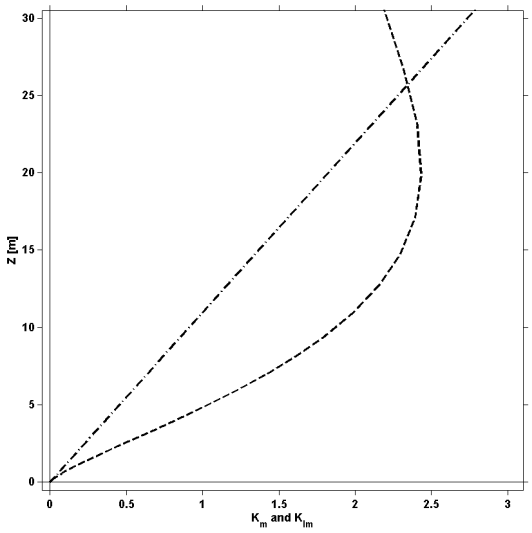

Figure 2 . Vertical profiles of the two eddy viscosity profiles, with TKE, K_m (dashed line) and linear, K_{lm} (dashed line).

The vertical profiles of the total stress and its components (turbulent and wave-induced stresses) for the K_{lm} formulation (related to the dot-dashed wind profile in figure 1), are plotted in figure 3. In this figure the total stress (vertical full line) is constant with height, and the wave-induced stress

(dashed line) is evaluated using the input parameters from equations (12) and (17). The turbulent stress (dot dashed line) is computed from $\tau_{turb} = \tau_{tot} - \tau_{wave}$. The decaying turbulent stress is related to the shape of the wind profile. Below the height of wind maximum the wind gradient is positive, but the wind shear is decaying. At the exact height of the wind maximum there is no wind shear, corresponding to the height where $\tau_{turb} = 0$. Above the height of the wind maximum the wind gradient becomes negative, driving a negative wind shear and consequently a negative turbulent stress.

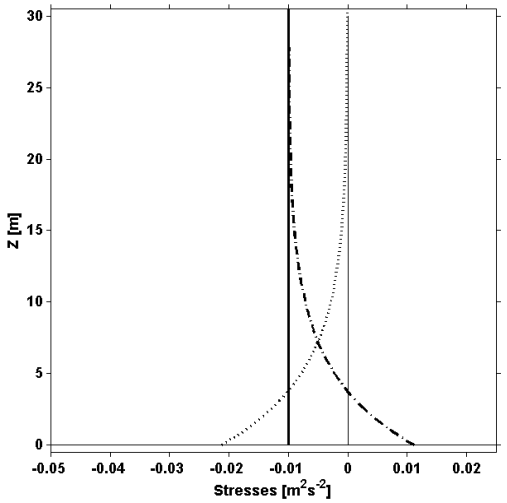

Figure 3. Vertical profiles of the total stress, constant (full line), wave-induced stress (dotted line), and turbulent stress (dot-dashed line). The height where $\tau_{turb} = 0$ corresponds to the height of the maxima on both modeled profiles on figure 1.

Model sensitivity tests to the variability of the wave damping parameter, the wave slope and the roughness length (using the model formulation from equation (22)), are performed. The model response to variations of β is shown in figure 4. The original profile with $\beta = 5 \times 10^{-5}\, s^{-1}$ is shown as a full line. The wave damping parameter was then varied ($\Delta\beta = 3 \times 10^{-6}\, s^{-1}$) keeping all the remaining parameters unchanged. Increasing values of β, corresponding to a higher loss of energy from the waves into the atmosphere, lead to higher wind speeds and to a raise in the height of the wind maxima (wind profiles in dashed lines on figure 4. The opposite effect, with lower values of β and consequently less energy loss from the waves lead to lower wind speeds and to lower heights of the wind maxima. The horizontal shift of the wind profiles on figure 4 occurs due to the fact that only β is varied and all the remaining parameters are kept unchanged, which is in a way unphysical, since the wave damping is a function of several parameters, mainly the wave field characteristics (wave phase speed and slope).

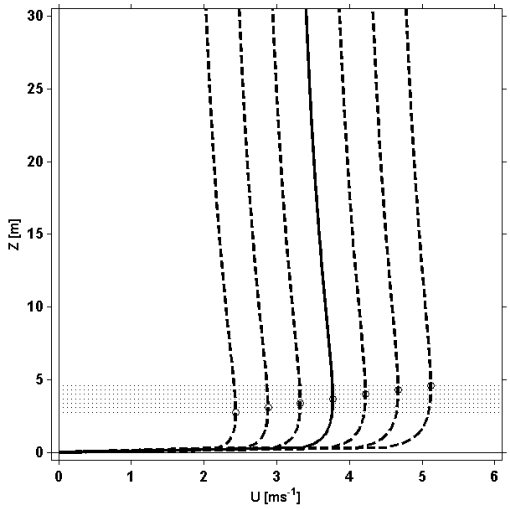

Figure 4. Model sensitivity tests to β variations. The circles represent the height of the wind maxima. The full line is the reference profile, with the original value of the wave damping parameter ($\beta = 5 \times 10^{-5}\, s^{-1}$). The dashed line profiles represent the wind profiles resulting from variations of β ($\Delta\beta = 3 \times 10^{-6}\, s^{-1}$).

The model response to wave slope variations is evaluated in a similar manner as for the β variations. The original profile computed with a wave slope $ak=0.1$ is shown as full line on figure 5, and the model response to wave slope variations ($\Delta ak = 5 \times 10^{-3}$) is then evaluated, keeping in mind that steeper waves will perform more work on the atmosphere than more gentle ones. The wave slope is varied having the remaining parameters constant.

For increasing values of wave slope, corresponding to steeper waves, higher wind speeds and higher wind speed maxima (wind profiles in dashed lines on figure 5) are generated. Less steep waves, lead to lower wind speeds lower heights of the wind speed maxima. The horizontal shifting of the wind profiles has the same explanation as for β variations.

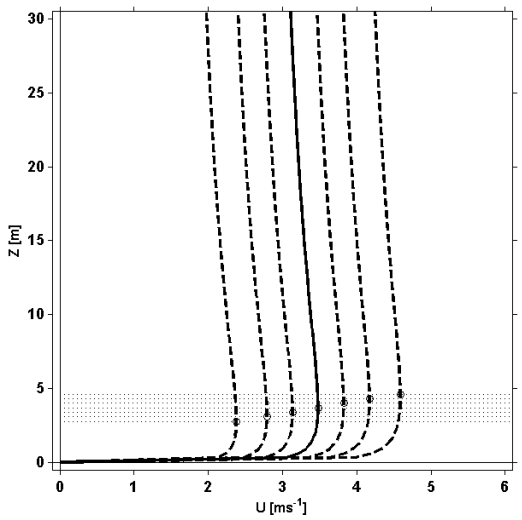

Figure 5. Model sensitivity tests to wave slope variations. The circles represent the height of the wind maxima. The full line is the reference profile, with the original value of the wave slope parameter ($ak = 0.1$). The dashed lined profiles represent the wind profiles resulting from variations of wave slope ($\Delta ak = 5 \times 10^{-3}$).

The fact that the wind profile over the ocean, under swell conditions, is no longer logarithmic makes the correct evaluation of the roughness length a cumbersome problem (Smedman et al. 2003, their figures 3 and 7). For the model sensitivity tests to roughness length variations several formulations are used (table 1). The profile using the Charnock (1955) formulation is taken as a reference and is shown as a full line. The remaining plots are shown as dashed lines. The effect of roughness length variations was different than the one obtained with the variations of β and the wave slope. The impact is no longer caused by the wave-induced part of equation (22) (second term on the right-hand side), but by the logarithmic component of the profile. Variations of z_0 will therefore lead to variation on the wind speed only, and not on the height of the wind speed maxima, as can be seen in figure 6. Larger values of z_0 will give rise to lower wind speed values, and the opposite to higher wind speed values.

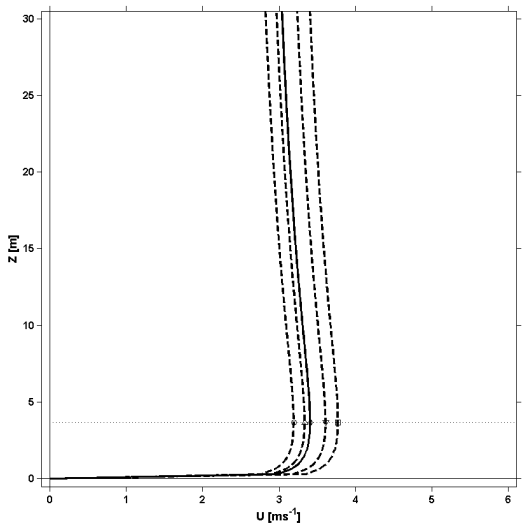

Figure 6. Model sensitivity tests to roughness length variations. The wind profile with the Charnock (1955) formulation, is taken as the reference profile (full line and diamond at the wind maximum). The remaining formulations (from table 1.), represented in dashed lines, are the Kudryavtsev and Makin (2004) formulation (circle), the Maat et al. (1991) formulation (triangle), the Donelan (1990) formulation (inverted triangle), and the Smith et al. (1992) formulation (square).

Table 1. Aerodynamical roughness length formulations used on the model sensitivity tests to the variability of z_o .

Reference	*Formulation*
Kudryavtsev and Makin (2004)	$z_o = (0.1\nu / u_*) + (0.012 u_*^2 / g)$
Maat et al. (1991)	$z_o = 0.8 u_*^2 (u_* / c_p)^{1.0}$
Charnock (1955)	$z_o = \alpha u_*^2 / g$
Doneland (1990)	$z_o = 1.84 \sigma (u_* / c_p)^{2.53}$
Smith et al. (1992)	$z_o = 0.48 u_*^2 (u_* / c_p)^{1.0}$

4. Summary

The model presented in the present study reproduced quantitatively and qualitatively the swell effect on the atmospheric flow, namely the generation of

a wave-induced wind and a wind maximum. The height of the maxima is in good agreement (same order of magnitude) with the most recent field observations and LES findings.

Acknowledgements

Alvaro Semedo is funded by the European Commission through a research fellowship under the ModObs project, contract MRTN-CT-2005-019369. Øyvind Saetra is partly funded by The Research Concil of Norway trough the project ArcChange, contract 178577/S3.

References

Anctil, F., M. Donelan, W. Drennan, and H. Graber, 1994: Eddy correlation measurements of air-sea fluxes from a discus buoy. *J. Atmos. Oceanic Tech.*, **11**, 1144–1150.

Belinov, A. Y., O. A. Kuznetsov, and G. N. Panin, 1974: On the analysis of wind-wave induced disturbances in the atmospheric tubulent surface layer. *Bound. Layer Meteor.*, **6**, 269–285.

Davidson, K. L. and A. J. Frank, 1973: Wave-related fluctuations in the airflow above natural waves. *J. Phys. Oceanogr.*, **3**, 102–119.

Donelan, M. A., W. M. Drennan, and K. B. Katsaros, 1997: The air-sea momentum flux in conditions of wind sea and swell. *J. Phys. Oceanogr.*, **27**, 2087–2099.

Drennan, W., M. Donelan, N. Madsen, K. Katsaros, E. Terray, and C. Flagg, 1994: Directional wave spectra from a swath ship at sea. *J. Atmos. Oceanic Tech.*, **11**, 1109–1116.

Graber, H. C., E. A. Terray, M. A. Donelan, W. M. Drennan, J. C. VanLeer, and D. B. Peters, 2000: Asis – a new air-sea interaction spar buoy: design and performance at sea. *J. Atmos. Oceanic Tech.*, **17**, 708–720.

Grachev, A. A. and C. W. Fairall, 2001: Upward momentum transfer in the marine boundary layer. *J. Phys. Oceanogr.*, **31**, 1698–1710.

Harris, D. L., 1966: The wave-driven wind. *J. Atmos. Sci.*, **23**, 688–693.

Högström, U., E. Sahlée,W.M. D. K. K., Kahma, A.-S. Smedman, C. Johansson, H. Pettersson, A. Rutgersson, L. Tuomi, F. Zhang, and M. Johansson, 2008: Momentum fluxes and wind gradients in the marine boundary layer a multi platform study. *Accepted in Boreal Env. Res.*, **00**, 00–00.

Hristov, T. S., S. D. Miller, and C. A. Friehe, 2003: Dynamical coupling of wind and ocean waves through wave-induced air flow. *Nature*, **422**, 55–58.

Janssen, P., (Ed.) , 2004: *The Interaction of Ocean Waves and Wind*. Cambridge Univeristy Press.

Kitaigorodskii, S. A., (Ed.) , 1970: *The Physics of Air-Sea Interaction*. Hydrometeoizdat
Leningrad, 284 pp. (Translated from Russian by A. Baruch, Israel Program for Scientific
Translations,1973, 273 pp.).

Kraus, E. B. and J. A. Businger, (Eds.) , 1994: *Atmosphere-Ocean Interaction*. Oxford Univerisity Press.

Kudryavtsev, V. N. and V. K.Makin, 2004: Impact of swell on the marine atmospheric boundary layer. *J. Phys. Oceanogr.*, **34**, 934–948.

Miles, J. W., 1957: On the generation of surface waves by shear flows. *J. Fluid Mech.*, **3 (4)**, 185–204.

Miller, S., C. Friehe, T. Hristov, j. Edson, and S. Wetzel, 1999: *Wind-over-wave couplings*, chap. Wind and turbulent profiles in the surface layer over ocean waves, 91–98. Calderon Press.

Phillips, O. M., (Ed.) , 1977: *The dynamics of the upper ocean*. Cambridge Univeristy Press. Rutgersson, A., A.-S.

Smedman, and U. H¨ogstr¨om, 2001: Use of conven-tional stability parameters during swell. *J. Geophys. Res.*, **106**, 27 117–27 134. 14

Rutgersson, A. and P. P. Sullivan, 2005: The effect of idealized water waves on the turbulence structure and kinetic energy budgets in the overlying airflow. *Dyn. Atmos. Oceans*, **38**, 147–171.

Saetra, Ø., 1998: Effects of surface film on the linear stability of an air-sea interface. *J. Fluid Mech.*, **357**, 59–81.

Smedman, A., X. G. Larsen, U. Högström, K. K. Kahma, and H. Pettersen, 2003: Effect of sea state on the momentum exchange over the sea during neutral conditions. *J. Geophys. Res.*, **108**, 1–13.

Smedman, A., U. Högström, H. Bergström, A. Rutgersson, K. K. Kahma, and H. Petterseon, 1999: A case study of air-sea interaction during swell conditions. *J. Geophys. Res.*, **104**, 25 833–25 851.

Smedman, A., M. Tjernström, and U. Högström, 1994: The Near-Neutral Marine Atmospheric Boundary Layer with No Surface Shearing Stress: A Case Study. *J. Atmos. Sci.*, **51**, 3399–3411.

Snodgrass, F. E., G.W. Groves, K. F. Hasselmann, G. R.Miller,W. H.Munk, and W. H. Powers, 1966: Propagation of Ocean Swell across the Pacific. *Phil. Trans. Roy. Soc. London*, **259A**, 431–497.

Sullivan, P. P., 2002: Turbulent flow over water waves in the presence of stratification. *Phys. Fluids*, **14**, 1182–1195.

Sullivan, P. P., J. B. Edson, T. Hristov, and J. C. McWilliams, 2008: Large-eddy Simulations and Observations of Atmospheric Marine Boundary Layers above Non-equilibrium Surface waves. *J. Atmos. Sci.*, In press. 15

Tennekes, H. and J. L. Lumley, 1972: *A first course in turbulence*. MIT Press, Cambridge.

Volkov, Y. A., 1970: Turbulent flux of momentum and heat in the atmospheric surface layer over a disturbed sea-surface. *Izv. Acad. Sci. USSR, Aatmos. Ocean. Phys. (Engl. Transl.)*, **6(12)**, 734–770.